

Verification of the Ramberg-Osgood Material Model in Midas GTS NX with the Modeling of Torsional Simple Shear Tests

Zsolt Szilvagyi^{1*} and Richard P. Ray¹

RESEARCH ARTICLE

Received 25 June 2017; Revised 02 October 2017; Accepted 09 January 2018

Abstract

This study focuses on the back analysis of a geotechnical laboratory test with nonlinear finite element modeling using the Ramberg-Osgood material model. This model has been used by several authors recently for nonlinear ground response analysis and it has been implemented by Midas into their commercial finite element code Midas GTS NX 2014. The verification of the model for 1D nonlinear site response analysis can be found in the documentation of the software package. In this study, Torsional Simple Shear tests were modeled and a comprehensive study was performed to provide verification of the material model for static torsional loading and axisymmetric conditions.

Keywords

Ramberg-Osgood model, Torsional Simple Shear Test, small strain stiffness

1 Introduction

Recently the importance of numerical modeling in geotechnical engineering has increased greatly; not only in research, but in everyday practice as well. As a result, geotechnical material models have developed tremendously due to their increased use with ever more complex design projects. While advances in computer technology have made this possible; the many economic and practical advantages of faster and more accurate solutions have made it a reality. The cycle time between research, development, deployment, and design implementation has indeed been reduced from years to months.

Since the deployment cycle has shortened, the process of verification and validation are even more crucial [1]. For geotechnical finite element software, verification is the process of showing that a model or method has been properly implemented in a computer program; while validation makes plausible that a computer model possesses the essential features to analyze a real world problem with results that are representative for the situation. The former is usually done by the software developer and the latter should be done by the user when creating a model. This paper focuses on the verification of the Ramberg-Osgood model in an axisymmetric case for static torsional loading. Laboratory tests have been performed on dry sand samples and results are used to verify the capabilities of the material model.

2 Small strain stiffness of soils

Many studies have shown that the accurate modeling of stiffness degradation with strain (and stress) is a key aspect in many dynamic as well as static geotechnical numerical calculations (e.g. earthquake vibrations, high speed railway induced vibrations, settlement calculations around retaining walls or tunnels etc.). It has been recognized [2], that soils behave linear-elastically only at very low strains (10^{-6} or 10^{-4} %) and as the strains (and stresses) increase, the initially constant shear stiffness or small strain stiffness (G_{max} or G_0) decreases gradually, as shown in Fig 1, while the damping or hysteretic behavior becomes more pronounced.

¹ Department of Structural and Geotechnical Engineering,
Faculty of Architecture, Civil Engineering and Transport Sciences,
Szechenyi Istvan University
H-9026 Gyor, Egyetem sqr. 1, Hungary

* Corresponding author, email: szilvagy@sze.hu

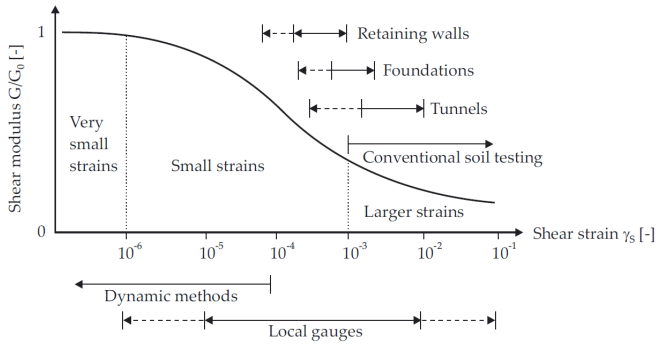


Fig. 1 Stiffness degradation of soil with typical strain ranges after [3]

A detailed discussion is presented in [4] about the small strain stiffness of soils, where first the historical development of elastic theory and the constitutive frameworks for its use in soil modeling is elaborated. Later the author shows how the comprehensive theoretical description of anisotropic elasticity can be simplified for practical calculations regarding soils. It should be emphasized, that beside anisotropy, several other factors have an effect on both the small strain stiffness and stiffness at larger strains.

The most important factors that affect small strain stiffness are:

- void ratio,
- grain properties (grain size and shape),
- effective overburden stress,
- stress history,
- rate of loading,
- structure and fabric of soil,
- discontinuities.

Factors that control the degradation of stiffness at larger strains are:

- strain level,
- loading path (change in effective stress),
- destructuring,
- change in rate of loading.

Some of these factors can be assessed by state of the art laboratory investigations e.g. Torsional Simple Shear (TOSS), [5], Resonant Column [6], [7], or Bender Element [8] testing. Results of such investigations are used to improve existing material models or create new models, which represent more aspects of the real behavior than earlier ones. Numerical models can then be used to investigate some of the factors mentioned.

3 Formulation of the Ramberg-Osgood model in Midas GTS NX

For cyclic and dynamic modeling the software Midas GTS NX offers several material models which are capable of modeling hysteretic behavior, but only two of them have been implemented for solid and axisymmetric solid elements which are used to model soil layers; the modified Ramberg-Osgood model and the modified Hardin-Drnevich model [9].

The Ramberg-Osgood model [10] was originally introduced for describing stress-strain curves of aluminum-alloy and steel sheets. The model used three parameters to define nonlinear stress-strain behavior, based on initial material stiffness, yield stress, and the rate of transition from linear behavior to full yielding. Later [11] adapted the model to generate nonlinear stress strain behavior and the concurrent shear modulus reduction and damping behavior for soil. The formulation has been modified to various ways [12], [13], and these models are called modified Ramberg-Osgood model. While the expressions are different from the original paper, all modified models are essentially identical. Since then, several authors used the model connected to geotechnical earthquake engineering e.g. [14].

The formulation by Midas uses the main equation for initial loading as:

$$G_0 \gamma = \tau \left(1 + \alpha |\tau|^\beta \right). \quad (1)$$

In (1) G_0 is the initial or small strain stiffness (shear modulus), γ and τ are shear strain and shear stress respectively, α and β are model parameters given by:

$$\alpha = \left(\frac{2}{\gamma_r G_0} \right)^\beta \quad \text{and} \quad \beta = \frac{2\pi h_{max}}{2 - \pi h_{max}}. \quad (2)$$

In (2) γ_r is the reference shear strain and h_{max} is the maximum damping constant.

For unloading and reloading the hysteresis curve is as follows:

$$G_0 \left(\frac{\gamma \pm \gamma_1}{2} \right) = \left(\frac{\tau \pm \tau_1}{2} \right) \left(1 + \alpha \left(\frac{\tau \pm \tau_1}{2} \right)^\beta \right). \quad (3)$$

In (3) γ_1 and τ_1 are the shear strain and stress values at the turnaround point, as shown in Fig. 2.

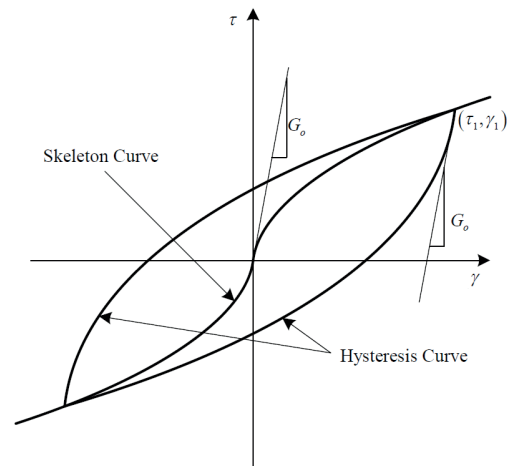


Fig. 2 Hysteresis loop of the Ramberg-Osgood model

4 Torsional Shear and Resonant Column Tests

A combined Resonant Column-Torsional Simple Shear device (RC-TOSS) designed and built by the authors, was used for testing [15], [14]. It has been further developed and used in previous studies at Széchenyi István University (SZE) [16], [17] and [18]. The benefit of the combined testing is that small strain stiffness

G_0 , small strain damping, large strain stiffness and damping can all be determined by two independent means on the same specimen in the same test. Additionally, arbitrary (earthquake) load histories or resonant and cyclic tests can be performed with an initial static torsional load applied. Both measurements can be performed on the same specimen over a wide range of strains and results can be checked against each other.

The device has a fixed-free configuration with the hollow cylinder (ID = 4cm, OD = 6cm, L = 14cm) sample connected rigidly to a base platen. The loading system, consisting of a top cap, suspension rod, drive head and two neodymium magnets rests on top of the specimen. It is free to rotate without restriction, see Fig. 3 and the weight of the system is counterbalanced by a vertical spring.

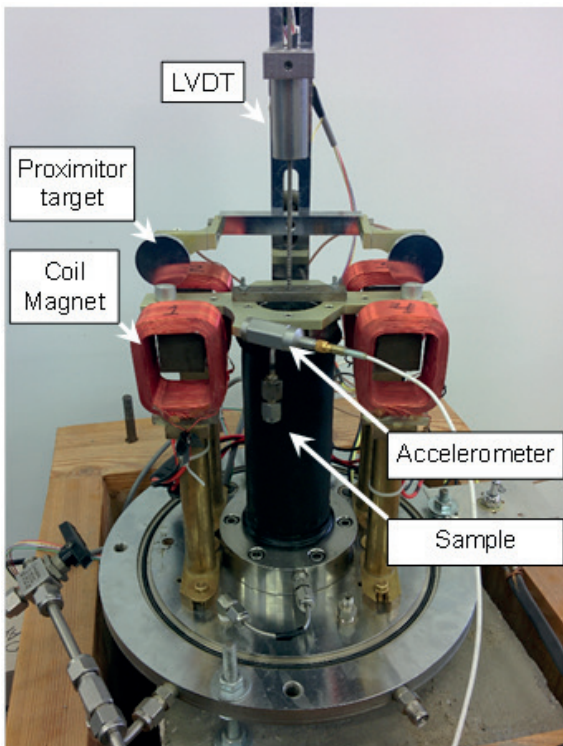


Fig. 3 Resonant Column-Torsional Simple Shear device with hollow cylinder sample

The magnets are individually surrounded by coils (in red color in Fig. 3) but they are free to move, therefore the sample is freely rotating around the vertical axis of the sample when a regulated flow of electricity in the coils causes the magnets to move. Hollow cylindrical samples are used for testing to insure a more even distribution of induced shear stresses and strains in the sample. For this comparative study, results of a combined RC-TOSS test performed on a dry sand were used. The specimen was prepared by dry pluviation from a height of 50 cm. Vacuum confinement of 84kPa was applied to the specimen during the assembly of the drive head and setup of measurement system. During the RC test, an accelerometer was used for measuring rotational acceleration of the top of the sample. For the TOSS test, a pair of proximitors measured

gap distances on two steel targets fixed on the drive head. An LVDT was mounted on the support rod to determine any vertical movement during testing. Stress controlled testing was used while strain controlled testing is under development. Over 200 tests have been performed at SZE in the past several years.

Some selected results of the combined test are shown in Fig. 4 and Fig. 5. The agreement between RC and TOSS test results is excellent, measured points clearly define a single degradation curve. Hysteresis loops of subsequent tests at different shear stress levels can be seen in Fig 5.

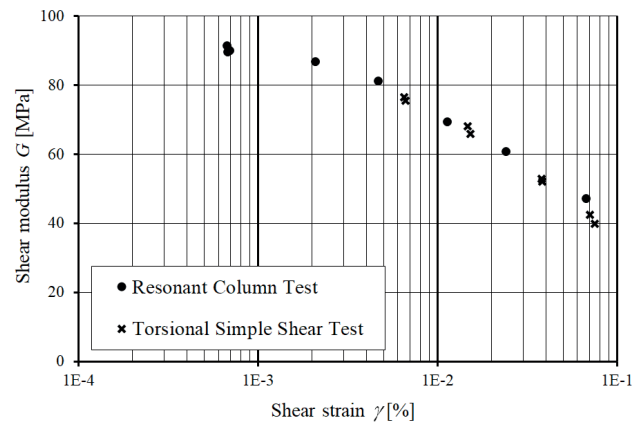


Fig. 4 Modulus reduction curve obtained with Resonant Column-Torsional Simple Shear device

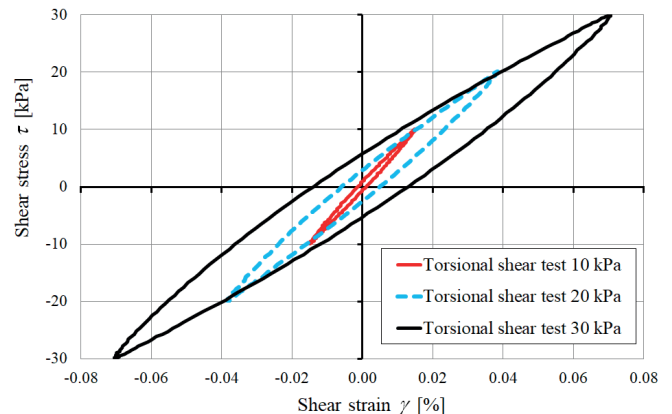


Fig. 5 Hysteresis loops of Torsional Shear tests at different stress (strain) levels

5 Modeling

5.1 General modeling aspects

Finite element modeling of such tests is a challenge. Since the geometry of the test is fundamentally axisymmetric, a realistic 3D model can be generated only by software capable of handling axisymmetric coordinate systems. An extended 2D (or 2.5D) axisymmetric model cannot be used, since the torsional load must be defined perpendicular to the model plane which is not possible, hence a true 3D model is required.

In Midas GTS NX axisymmetric 3D modeling can be performed by either defining a global cylindrical coordinate system or using the cylindrical element coordinate system. For this study the latter was used. Fig. 6 shows a part of the model with the finite element mesh. Hexahedral high order elements

with 20 nodes were used with an average size of $4 \times 4 \times 3$ mm. Nodes on the grey soil elements can be seen in blue in Fig. 6. This mesh was chosen so that three layers of elements would build up the cross section and so strain distribution could easily be assessed within the 1 cm thick hollow cylinder. More refined meshes were studied with little increase in accuracy.

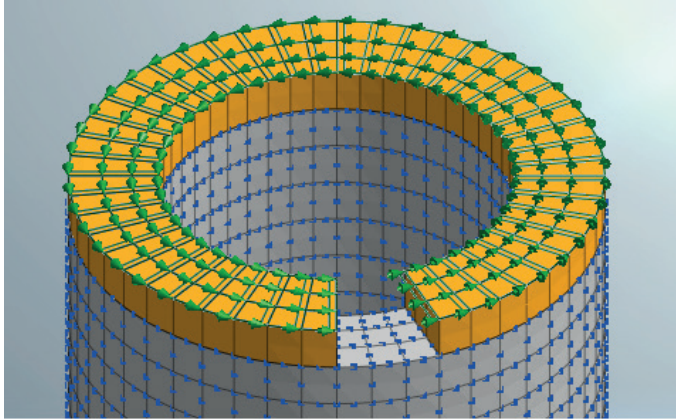


Fig. 6 Detail of finite element mesh of soil sample and steel ring (partially not shown)

Fig. 6 also shows yellow elements on top of the hollow cylinder soil sample, representing the steel ring which transfers the load to the soil sample. A part of this ring is switched off to better show soil elements. The imposed torsional load is modeled as surface stress acting in the rotational direction of the axisymmetric element coordinate system. Without this option, an imposed node load would act in a continuing tangential direction, which does not reflect the true behavior in this case.

The mesh consisted of 4032 elements. More refined meshes showed similar results, while an even coarser mesh with one layer of high order elements, with a total number of 162 elements showed identical results of overall specimen behavior.

Pinned boundary conditions were used on the bottom surface of the soil sample since in the test the soil directly connects to the rough surface of the porous stone. It should be noted that some stress irregularities were observed even in the fine mesh close to the base fixity when using fully fixed boundary conditions (fixed against translation and rotation in each direction). The irregularities with pinned fixities were minor, see Fig. 7. Since the testing device is free on top and the self-weight of the drive head is counterbalanced by a calibrated vertical spring, no other fixities have to be introduced in the model.

Calculation stages consisted of initial stress generation, confinement activation (with free face surface pressure acting in normal direction of the element faces) and torsional loading stages. This can be done in the software by defining construction stage sets and setting up construction stage analysis cases. Another important modeling step is to define output control before starting the calculation. Small sub-sets of the mesh can be chosen for documenting stress, strain, etc. While

the calculation will be performed for the whole mesh, results will only be saved for these selected elements, significantly reducing output data storage requirements. This still might be crucial for 3D FEM calculations since one time history result could occupy several gigabytes of storage. With such a large data set, analyzing results were slowed significantly and inevitably led to hard drive capacity issues. Result types (deformation, stress, strain) can also be set before analysis. Oddly, Midas software does not record element strains by default which can lead to some initial confusion for new users.

Formulation of the material model has been presented in Chapter 3. An additional modeling detail in Midas is that the user can specify using the model in “shear only” mode; which was done in this study. Unfortunately, the effects of this option are not detailed in the manual, however the online release notes explain that if this mode is used, shear modulus will be different in each direction separately (G_{xy} , G_{yz} , G_{zx}), otherwise an equivalent shear modulus will be used (G_{eq}). While this information is somewhat helpful, there seems to be no way of inputting separate shear moduli for each direction and the formulation of G_{eq} is also not part of the manual as of the time of modeling.

5.2 Back analysis of model parameters

Obtaining soil parameters for FEM models from various laboratory and field tests is also a challenging task because it involves the solution of an inverse problem. Some geotechnical FEM software offer built-in program modules for fitting curves of commonly used laboratory tests, (e.g. Soil Test module in Plaxis), so that the user can assess the effects of changing a single parameter and chose the most appropriate set of parameters for the specific project. However, laboratory tests such as the Resonant Column or Torsional Shear Test are not yet implemented in any of the mentioned modules.

For this study, in order to obtain model parameters, the G_0 value measured in low strain Resonant Column tests and the stress-strain values of a higher strain single hysteresis loop obtained with the Torsional Shear test were used. The measurement results were imported into MS Excel and the formulation of the material model was implemented into a Visual Basic code. Then, with a set of initial values for γ_r and h_{max} the response of the model was calculated. Due to the properties of the formulation, if a full hysteresis loop is used, the turnaround point has to be specified in advance as well. Then, at each data point, the square of the error between measured and computed by the RO model could be obtained and sum of the error squares could be calculated. In MS Excel, the Solver module was then used to choose model parameters with the best fit, namely the nonlinear GRG method (Generalized Reduced Gradient) was applied to minimize the sum of square of the errors by allowing Solver to change the two model parameters and solve the inverse problem. The obtained model parameters are summarized in Table 1.

Table 1 Ramberg-Osgood material model parameters used in this study

Parameter		Value	Dimension
Small strain stiffness from RC test	G_0	91 161	kPa
Reference shear strain*	γ_r	$8.137 \cdot 10^{-4}$	-
Max. damping constant*	h_{max}	0.19043	-
Dry density	γ_d	16.15	kN/m ³
Poisson's ratio	ν	0.3	-

*Parameters modified by Solver for obtaining best fit

From a practical viewpoint; the GRG method works best if the fitting parameters are of the same order of magnitude. This can be achieved by adjusting the options in Solver.

Several shear stress levels were defined in the program up (10 to 90kPa), so calculation was also stress controlled, as the laboratory test itself.

6 Results

Horizontal stresses after the 84kPa confinement step are shown in Fig. 7. Some minor irregularities can be observed close to the base fixities. However, the difference is less than 1%.

A one-way loading stress-strain curve is shown in Fig. 8. Stress and strain values were taken as the average of three layers of elements in the cross section. This average was found to be almost identical to the value in the middle element. Response of the inside element and the outside element follow the same stress strain curve closely, see Fig. 8.

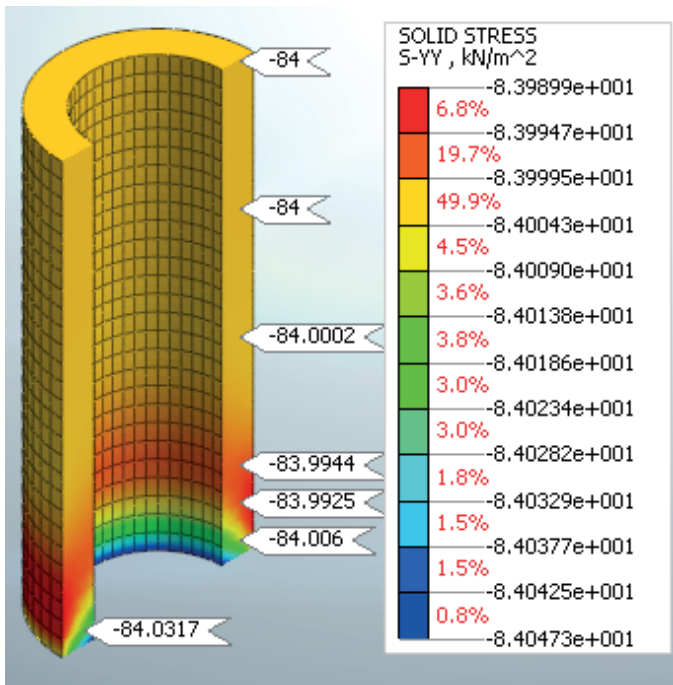


Fig. 7 Distribution of horizontal normal stresses after confinement activation

Agreement between the formulation and the FEM calculation is nearly exact, see Fig. 9.

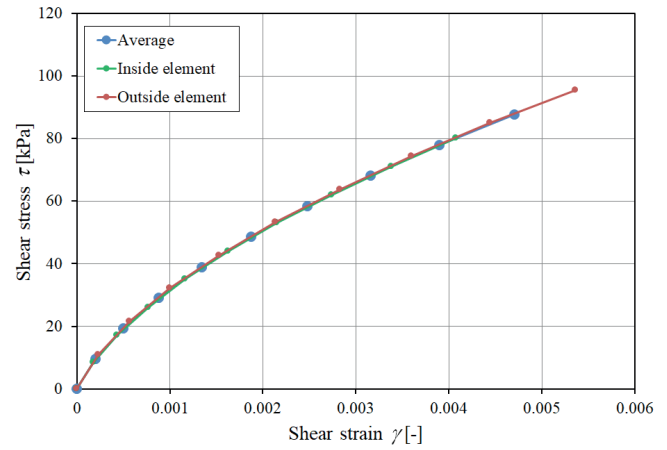


Fig. 8 Comparison of shear stresses in cross section

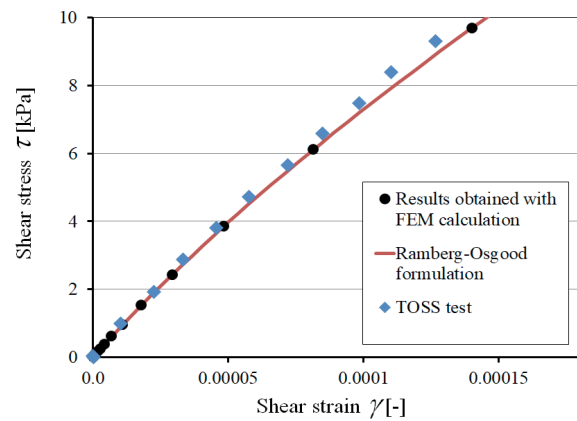


Fig. 9 Stress-strain curve by FEM calculation and MIDAS Ramberg-Osgood formulation compared to laboratory test

The calculations were performed at several shear stress levels and based on the obtained shear strain values, the secant shear modulus was calculated. Two-way loading was also applied. For this, manual load stepping was found to be beneficial as it resulted in more stable calculations than with automated load stepping. Load step size around turnaround points of the hysteresis loops should be gradually smaller to achieve a stable calculation. The developed manual load stepping sequence is shown in Fig. 10.

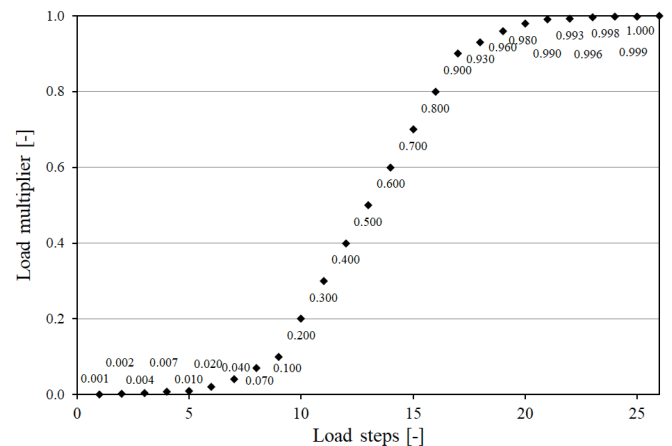


Fig. 10 Manual load stepping used for stable calculation of hysteresis loop

Hysteresis loops from the model overlap with the test results perfectly. Result of a single loop is shown in Fig. 11. This shows that the model can follow the numerically demanding load reversal problem accurately.

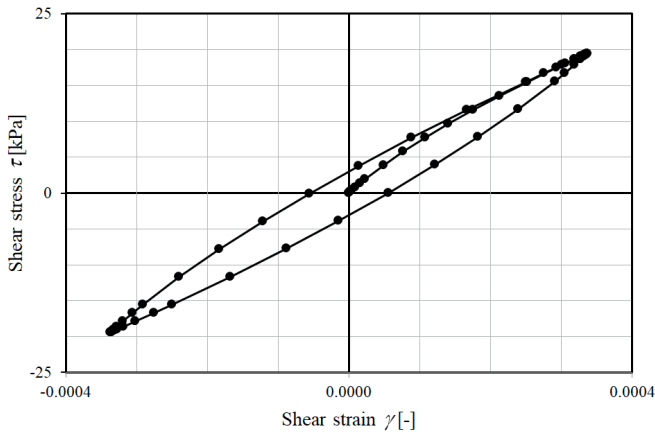


Fig. 11 Single hysteresis loop obtained with FEM calculation

A sequence of computed hysteresis loops can be seen in Fig. 12. They reflect the same behavior seen in testing (Fig. 5)

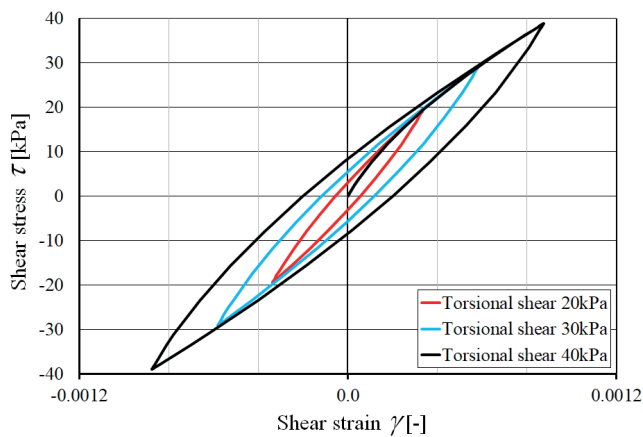


Fig. 12 Hysteresis loops obtained from two-way sequential loading with FEM calculation

Fig. 13 and Fig. 14 show the deformed mesh and the distribution of total deformations in the mesh. The horizontal shear of the elements is clearly observable.

As expected, the top of the soil cylinder moves the most, while there is no movement at the fixed base. The cross section also reveals that displacement distribution is also realistic in any horizontal plane, namely there is larger displacement at the outer rim of the cylinder than at the inner rim.

Fig. 15 shows shear strain distribution in the sample, which is uniform throughout the height of the sample. Also the benefit of using a hollow cylinder for testing is demonstrated here; strain difference within the sample ($\pm 20\%$ of average) would be considerably higher in a solid cylinder.

The calculations were performed at several shear strain levels and based on the obtained shear stress and strain values; the secant shear modulus was calculated. Fig. 16 shows the normalized modulus degradation curve compared to the test data.

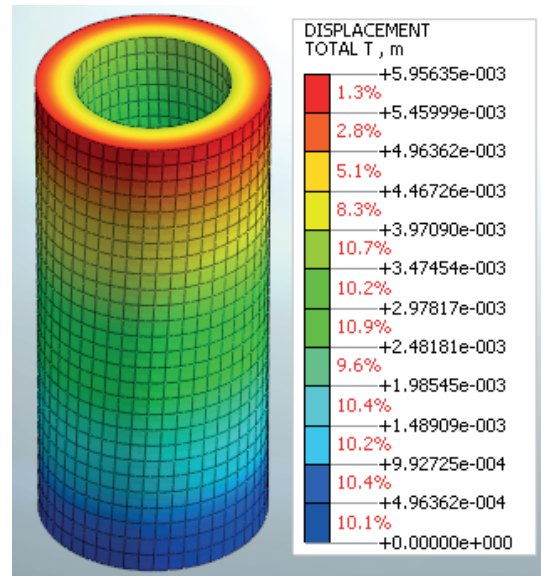


Fig. 13 Deformed mesh at turnaround point of loading

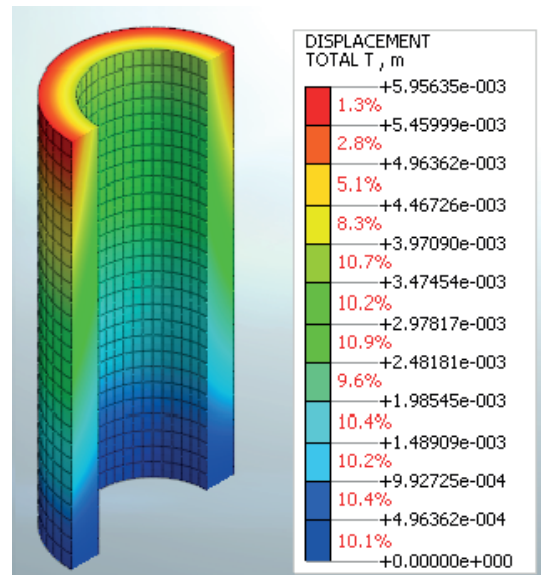


Fig. 14 Distribution of total displacements at turnaround point of loading

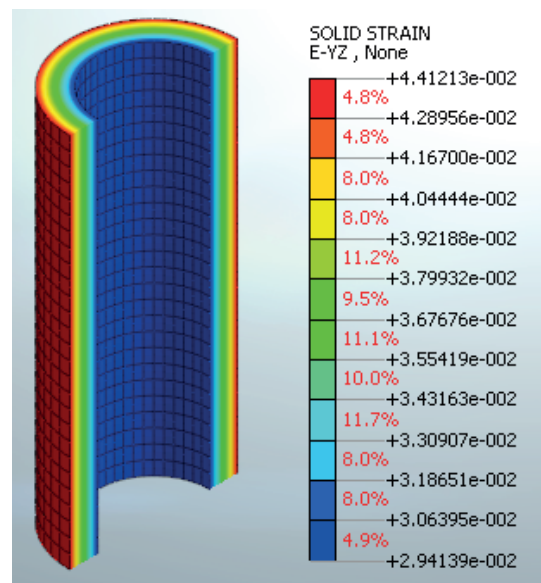


Fig. 15 Shear strain distribution at turnaround point of loading

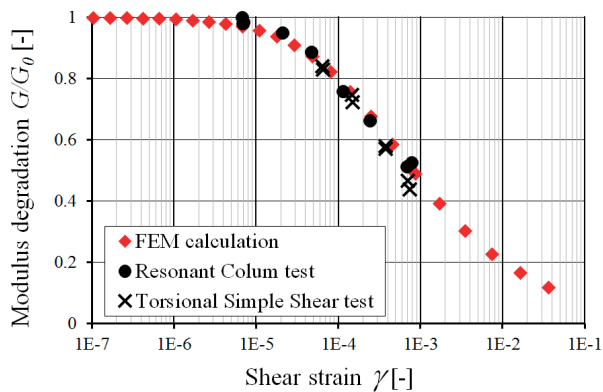


Fig. 16 Modulus reduction curve by FEM calculation and RC-TOSS tests

7 Conclusions

This study focused on the small strain stiffness and stiffness degradation of soils with increasing strain levels. Laboratory testing has been performed and the results of a numerical modeling study has been presented. It has been shown how the inverse problem can be solved to obtain material model parameters, which allow the model to reproduce the laboratory test results. By this modeling we have verified, that the Ramberg-Osgood material model implemented in MIDAS GTS NX v2014 is capable of modeling this static axisymmetric laboratory test with representation of nonlinear material behavior. Modulus degradation and hysteretic behavior was also captured by the model. Sequential two-way loading modeling showed very good agreement with test results.

Some minor modeling difficulties have been pointed out. The use of manual load stepping and smaller load step size before and after the turnaround point was found to be beneficial to achieve a stable calculation. This confirms the general expectation, that to calculate more complicated load histories, such as recorded earthquake load histories, a smaller load step size may be required when using automated load stepping.

Future studies will focus on more complicated load histories, modeling dynamic tests, the effects of minor irregularities in the sample on the stiffness.

References

- [1] Brinkgreve, R., Engin, E. "Validation of geotechnical finite element analysis". In: *Proceedings of the 18th International Conference on Soil Mechanics and Geotechnical Engineering*, Paris, France, ISSMGE TC 103, pp. 677–682. 2013. <http://www.issmge.org/uploads/publications/1/2/677-682.pdf>
- [2] Richart, F. "Some Effects of Dynamic Soil Properties on Soil-Structure Interaction". *Journal of the Geotechnical Engineering Division*, 101(12), pp. 1193–1240. 1975.
- [3] Atkinson, J. H., Salfors, G. "Experimental determination of soil properties". In: *Proceedings of the 10th European Conference on Soil Mechanics and Foundation Engineering*, Vol 3, Florence, 1991, pp. 915–956.
- [4] Clayton, C. R. I. "Stiffness at small strain: research and practice". *Géotechnique*, 61(1), pp. 5–37. 2011. <https://doi.org/10.1680/geot.2011.61.1.5>
- [5] Pradhan, T., Tatsuoka, F., Horii, N. "Simple Shear Testing on Sand in a Torsional Shear Apparatus". *Soils and Foundations*, 28(2), pp. 95–112, 1988. https://doi.org/10.3208/sandf1972.28.2_95

- [6] Yu, X., Sun, R., Yuan, X., Chen, Z., Zhang, J. "Resonant Column Test on the Frozen Silt Soil Modulus and Damping at Different Temperatures". *Periodica Polytechnica Civil Engineering*, 61(4), pp. 762–769. 2017. <https://doi.org/10.3311/PPci.10349>
- [7] Edinçliler, A., Cabalar, A., Cevik, A., Isik, H. "New Formulations for Dynamic Behavior of Sand-Waste Tire Mixtures in a Small Range of Strain Amplitudes". *Periodica Polytechnica Civil Engineering*, 62(1), pp. 92–101. 2018. <https://doi.org/10.3311/PPci.8698>
- [8] Jovičić, V. "The Measurement and Interpretation of Small Strain Stiffness of Soils". (Doctoral Thesis). City University, London, 1997, pp. 1–278. <http://openaccess.city.ac.uk/8268/>
- [9] MIDAS Information Technology Co., „*Midas GTS NX 2014 v2.1 Analysis Reference*". Chapter 4: Materials. pp. 105-211. 2014.
- [10] Ramberg, W., Osgood, W. R. "Description of stress strain curves by three parameters". *National Advisory Committee for Aeronautics, Technical Note*, No. 902. p. 28. 1943. <http://hdl.handle.net/2060/19930081614>
- [11] V. W. E. R. F. J. Streeter, "Soil Motion Computation by Characteristics Method". *Journal of the Geotechnical Engineering Division*, 100(3), pp. 247–263. 1974.
- [12] Ishihara, K. "Soil Behavior in Earthquake Geotechnics". Oxford University Press, New York, pp. 33–39. 1996.
- [13] Adachi, N., Tatsuoka, F. "Soil mechanics III - consolidation, shear and dynamic analysis". Gihodo, Tokyo, 1986.
- [14] Ray, R., Woods, R. "Modulus and damping due to uniform and variable cyclic loading". *Journal of Geotechnical Engineering*, 114(8), pp. 861–876. 1988. [https://doi.org/10.1061/\(ASCE\)0733-9410\(1988\)114:8\(861\)](https://doi.org/10.1061/(ASCE)0733-9410(1988)114:8(861))
- [15] Ray, R. P. "Changes in shear modulus and damping in cohesionless soils due to repeated loading, PhD Dissertation". University of Michigan, Michigan, USA, p. 417. 1983
- [16] Ray, R. P., SzilvÁgyi, Z., "Measuring and modeling the dynamic behavior of Danube Sands". In: *Proceedings 18th International Conference on Soil Mechanics and Geotechnical Engineering: Challenging and Innovations in Geotechnics*, Paris, Presses des Ponts, 2013, pp. 1575–1578. <http://www.cfms-sols.org/sites/default/files/Actes/1575-1578.pdf>
- [17] SzilvÁgyi, Z., Hudacsek, P., Ray, R.P. "Soil shear modulus from Resonant Column, Torsional Shear and Bender Element Tests". *International Journal of Geomate*, 10(20), pp. 1822–1827. 2016.
- [18] SzilvÁgyi, Zs., Panuska, J., Kegyes-Brassai, O., Wolf, Á., Tildy, P., Ray, R. P. "Ground Response Analyses in Budapest Based on Site Investigations and Laboratory Measurements". In: *Ground Response Analyses in Budapest Based on Site Investigations and Laboratory Measurements*, World Academy of Science Engineering and Technology, 2017, pp. 307–317. <http://scholar.waset.org/1999.6/10006887>
- [19] Idriss, I. M., Dobry, R., Singh, R. D. "Nonlinear behavior of soft clays during cyclic loading". *Journal of the Geotechnical Engineering Division*, 104(12), pp. 1427–1447. 1976.